ISSN 2070-2051, Protection of Metals and Physical Chemistry of Surfaces, 2016, Vol. 52, No. 2, pp. 348–355. © Pleiades Publishing, Ltd., 2016.

PHYSICOCHEMICAL PROBLEMS OF MATERIALS PROTECTION

# Electrochemical Investigation of Inhibitory of New Synthesized 3-(4-Iodophenyl)-2-imino-2,3-dihydrobenzo[*d*]oxazol-5-yl 4-methylbenzenesulfonate on Corrosion of Al in Acidic Medium[1]

**Ali Ehsani[a] and Hamid Mohammad Shiri[b]**

[a] *Department of Chemistry, Faculty of science, University of Qom, Qom, Iran*

[b] *Department of Chemistry, Payame Noor University, Iran*

*e-mail: ehsani46847@yahoo.com, a.ehsani@qom.ac.ir*

Received July 6, 2014

**Abstract**—3-(4-Iodophenyl)-2-imino-2,3-dihydrobenzo[*d*]oxazol-5-yl 4-methylbenzenesulfonate (4-IPhOXTs) was synthesized and its inhibiting action on the corrosion of Aluminum 1005 in sulfuric acid was investigated by means of potentiodynamic polarization and electrochemical impedance spectroscopy (EIS). The results of the investigation show that this compound has excellent inhibiting properties for Al corrosion in sulfuric acid. Inhibition efficiency increases with increase in the concentration of the inhibitor. The adsorption of 4-IPhOXTs onto the Al surface followed the Langmuir adsorption model with the free energy of adsorption $\Delta G^0_{ads}$ of −9.18 kJ mol$^{-1}$. Quantum chemical calculations were employed to give further insight into the mechanism of inhibition action of 4-IPhOXTs.

**DOI:** 10.1134/S2070205116020088

## 1. INTRODUCTION

Since Al and Fe and their alloys are the backbone of industrial constructions, many research projects have been concerned with their stability. One of most important tasks is the retardation of the attack by acid solutions used during pickling, industrial cleaning and descaling. The use of an additive is one of the major solutions for this problem. Hence, various additives are used to protect iron and its alloy against corrosive attack [1–5]. The use of organic molecules containing functional groups and p-electrons in their structure, as corrosion inhibitors, is one of the most practical methods for protecting metals against corrosion and it is becoming increasingly popular. The existing data show that organic inhibitors act by adsorption and they protect the metal by film formation. Organic compounds bearing heteroatoms with high electron density such as phosphorus, sulfur, nitrogen, oxygen or those containing multiple bonds which are considered as adsorption centers, are effective as corrosion inhibitors [6–10]. The compounds containing both nitrogen and sulfur in their molecular structure have exhibited greater inhibition compared with those possessing only one of these atoms [11–13]. In the literature, many thiazole derivatives have been reported as corrosion inhibitors and found to have good corrosion inhibition effect [14, 15]. The efficiency of an organic compound inhibitor is mainly dependent on its ability to adsorb on a metal surface, which consists of replacement of a water molecule at a corroding interface. In this study research methods including the weight loss method and electrochemical tests were employed to investigate the inhibition performance of new synthesized 4-IPhOXTs inhibitor in acidic solution. Quantum chemical calculations based on DFT method was performed on new compound used as corrosion inhibitor for Al in acid media to determine the optimized structural parameters, such as the frontier molecular orbital energy HOMO (highest occupied molecular orbital) and LUMO (lowest unoccupied molecular orbital).

## 2. EXPERIMENTAL

### *2.1. Materials and Apparatus*

The employed working electrodes with surface area of 3mm$^2$ were prepared from aluminum AA 1005 with composition of Al: 99.8, Ni: 0.6601, Si: 0.1, Mn: 0.006, Mg: 0.005, Cu: 0.01, Pb: 0.03, Bi: 0.005, Co: 67 0.002, Ti: 0.002, Na: 0.001, Fe: 0.05, andGa: 0.005(%wt). The exposed surface of Al was ground with silicon carbide abrasive paper from 400 to 1200, degreased with

[1] The article is published in the original.

absolute ethanol, rinsed in distilled water, and dried in warm air. The exposed surface was ground with silicon carbide abrasive paper from 400 to 1200, degreased with absolute ethanol, rinsed in distilled water, and dried in warm air. The corrosive medium was 0.5 M $H_2SO_4$ solution prepared from analytical reagent grade 98% sulfuric acid and distilled water. 3-(4-Iodophenyl)-2-imino-2,3-dihydrobenzo[*d*]oxazol-5-yl 4-methylbenzenesulfonate was synthesized in our laboratory from the reaction between 3-(4-iodophenyl)-2-imino-2,3-dihydrobenzo[*d*]oxazol-5-ol with *p*-toluenesulfonyl chloride and $K_2CO_3$ in EtOH under ultrasound irradiation for 2.5 h at room temperature. The crude product was purified by aqueous ethanol to afford the pure product (Yield 84%) and characterized by $^1$H NMR, $^{13}$C NMR, FT-IR, elemental analysis (CHN), and melting points. M.p. 199–201°C; FT-IR (KBr, cm$^{-1}$): 3344, 3043, 1704, 1496, 1480, 1355, 1170, 1132, 1092, 893, 857, 819, 753, 592, 553; $^1$H NMR (400 MHz, DMSO-$d_6$): $\delta_H$ = 7.89 (d, $J$ = 8.4 Hz, 2H), 7.72 (d, $J$ = 8.0 Hz, 2H), 7.36 (d, $J$ = 8.0 Hz, 3H), 7.24 (d, $J$ = 8.4 Hz, 2H), 7.09 (d, $J$ = 8.8 Hz, 1H), 6.66 (d, $J$ = 8.8 Hz, 1H), 6.58 (d, $J$ = 2.4 Hz, 1H), 2.50 (s, 3H); $^{13}$C NMR (100 MHz, DMSO-$d_6$): $\delta_C$ = 156.2, 145.7, 145.6, 142.9, 139.2, 133.7, 133.2, 131.9, 129.9, 128.7, 127.2, 116.0, 109.4, 103.6, 93.4, 21.8; CHN: Anal. Calcd for $C_{20}H_{15}IN_2O_4S$: C, 47.44; H, 2.99; N, 5.53. Found: C, 47.52; H, 3.10; N, 5.64.

The concentration range of 4-IPhOXTs employed was $1 \times 10^{-4}$ to $10^{-3}$ M in 0.5 M sulfuric acid. All electrochemical measurements were carried out in a conventional three electrode cell, powered by a potentiostat/galvanostat (EG&G 273A) and a frequency response analyzer (EG&G, 1025). The system was run by a PC through M270 and M398 software via a GPIB interface. The frequency range of 100 kHz to 15 mHz and modulation amplitude of 5 mV were employed for impedance studies. A Al electrode was employed as the working electrode. A saturated calomel electrode (SCE) and a platinum wire were used as reference and counter electrodes, respectively. Before measurement, the working electrode was immersed in test solution for approximately 1 h until a steady open circuit potential (OCP) was reached. The polarization curves were carried out from cathodic potential of –1.4 V to anodic potential of 0.10 V with respect to the open circuit potential at a sweep rate of 0.5 mV/s. The linear Tafel segments of the anodic and cathodic curves were extrapolated to corrosion potential ($E_{corr}$) to obtain the corrosion current densities ($i_{corr}$). In each measurement, a fresh working electrode was used. Several runs were performed for each measurement to obtain reproducible data.

### *2.2. Computational Details*

The use of quantum chemical calculations has become popular for screening new potential corrosion inhibitors [17]. Theoretical calculations were carried out at density functional theory (DFT) level using the 6-31*G* (d,p) basis set for all atoms with Gaussian 03 program package. Electronic properties such as highest occupied molecular orbital (HOMO) energy, lowest unoccupied molecular orbital (LUMO) energy and frontier molecular orbital coefficients have been calculated. The molecular sketches of all compounds were drawn using Gauss View 03 [18]. The natural bond orbital (NBO) analysis, suggested by Reed et al. [19, 20], was applied to determine the atomic charges.

## 3. RESULTS AND DISCUSSION

### *3.1. Potentiodynamic Polarization Studies*

Polarization measurements were carried out to get information regarding the kinetics of anodic and cathodic reactions. The potentiodynamic polarization curves for Al in 0.5 M $H_2SO_4$ solution in the absence and presence of different concentrations of the inhibitor molecules are shown in Fig. 1. The values of electrochemical kinetic parameters such as corrosion potential ($E_{corr}$), corrosion current ($I_{corr}$) and Tafel slopes, determined from these by extrapolation method, are listed in 1. In corrosion, quantitative information on corrosion currents and corrosion potentials can be extracted from the slope of the curves, using the Stern-Geary equation, as follows [21]:

$$i_{corr} = \frac{1}{2.303R_p}\left(\frac{\beta_a \times \beta_c}{\beta_a + \beta_c}\right), \quad (1)$$

$i_{corr}$ is the corrosion current density in Amps/cm$^2$; $R_p$ is the corrosion resistance in ohms cm$^2$; $\beta_a$ is the anodic Tafel slope in Volts/decade or mV/decade of current density; $\beta_c$ is the cathodic Tafel slope in Volts/decade or mV/decade of current density; the quantity, $\frac{\beta_a \times \beta_c}{\beta_a + \beta_c}$, is referred to as the Tafel constant. The corrosion inhibition efficiency was calculated using the relation:

$$\eta(\%) = 100\left(\frac{i^*_{corr} - i_{corr}}{i^*_{corr}}\right), \quad (2)$$

where $i^*_{corr}$ and $i_{corr}$ are uninhibited and inhibited corrosion current densities, respectively, determined by extrapolation of Tafel lines in the corrosion potential. The corrosion rates ν (mm year$^{-1}$) from polarization were calculated using the following Equation:

$$\upsilon = \frac{i_{corr} \times t \times M}{F \times S \times d} \times 10,$$

where $t$ is the time (s), $M$ is the equivalent molar weight of working electrode (g mol$^{-1}$), $F$ is Faraday constant (96500 C. mol$^{-1}$), $S$ is the surface area of

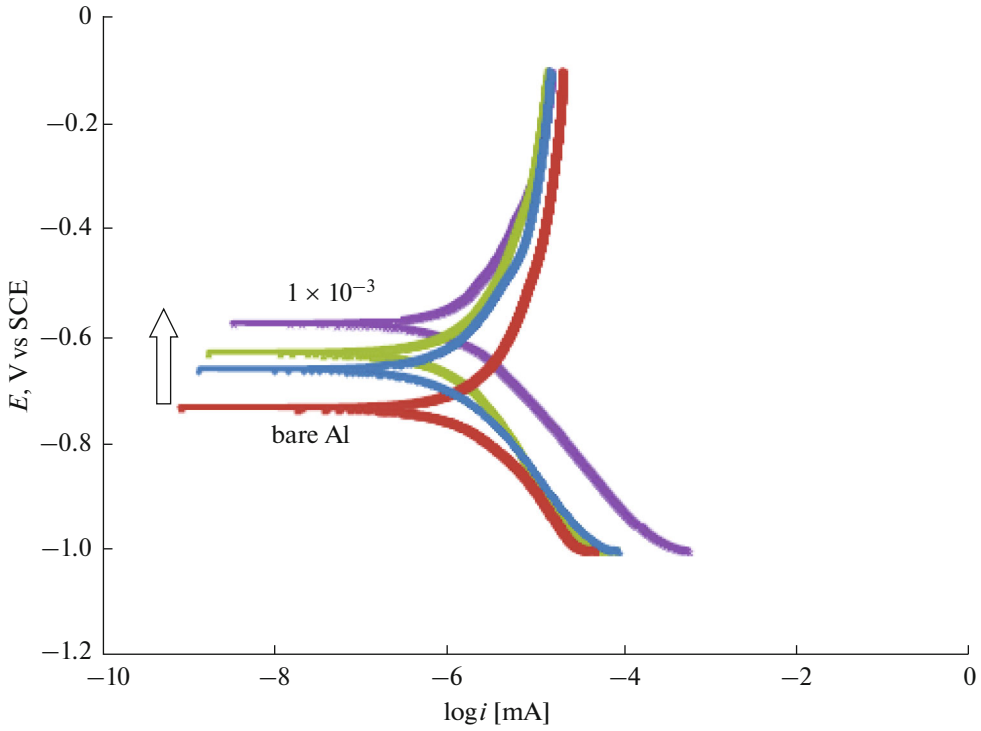


**Fig. 1.** Potentiodynamic polarisation curves of Al in 0.5 M $H_2SO_4$ solution in the absence and presence of various concentrations of the 1,4-$Ph(OX)_2(Ts)_2$.

electrode, *d* is the density of Al and the constant 10 is used to convert the unit cm to mm. The results are presented in Table 1. The inhibitor molecule first adsorbs on the Al surface and blocks the available reaction sites. As the concentration of the inhibitor increases, the linear polarization resistance (LPR) increases and corrosion Rate (CR) decreases. The surface coverage increases with the inhibitor concentration and the formation of inhibitor film on the Al surface reduces the active surface area available for the attack of the corrosive medium and delays hydrogen evolution and metal dissolution [22]. In the cathodic domain, as seen in Table 1, the values of βc show small changes with increasing inhibitor concentration, which indicates that the 4-IPhOXTsis adsorbed on the metal surface and the addition of the inhibitor hinders the acid attack on the Al electrode. In anodic domain, the value of βa decreases with the presence of 4-IPhOXTs. The shift in the anodic Tafel slope βa might be attributed to the modification of anodic dissolution process due to the inhibitor modules adsorption on the active sites. Compared to the absence of 4-IPhOXTs, the anodic curves of the working electrode in the acidic solution containing the 4-IPhOXTsclearly shifted to the direction of current reduction, as it could be observed from these polarization results; the inhibition efficiency

**Table 1.** Corrosion parameters obtained from Tafel polarisation curves of Al in 0.5M $H_2SO_4$ in the absence and presence of different concentrations of 4-IPhOXTsat 298 K

| No. | Inhi. Con. | $\beta_a$, v/decade | $\beta_c$, v/decade | *i*, uA | *E*, v |
|---|---|---|---|---|---|
| $Al_1$ | 0 | 0.43 | 0.17 | 2.56 | –0.73 |
| $Al_2$ | 0.001 | 0.41 | 0.26 | 2.06 | –0.69 |
| $Al_3$ | 0.002 | 0.38 | 0.36 | 1.85 | –0.66 |
| $Al_4$ | 0.004 | 0.35 | 0.21 | 1.58 | –0.67 |
| $Al_5$ | 0.006 | 0.31 | 0.22 | 1.38 | –0.65 |
| $Al_6$ | 0.008 | 0.27 | 0.22 | 1.08 | –0.61 |

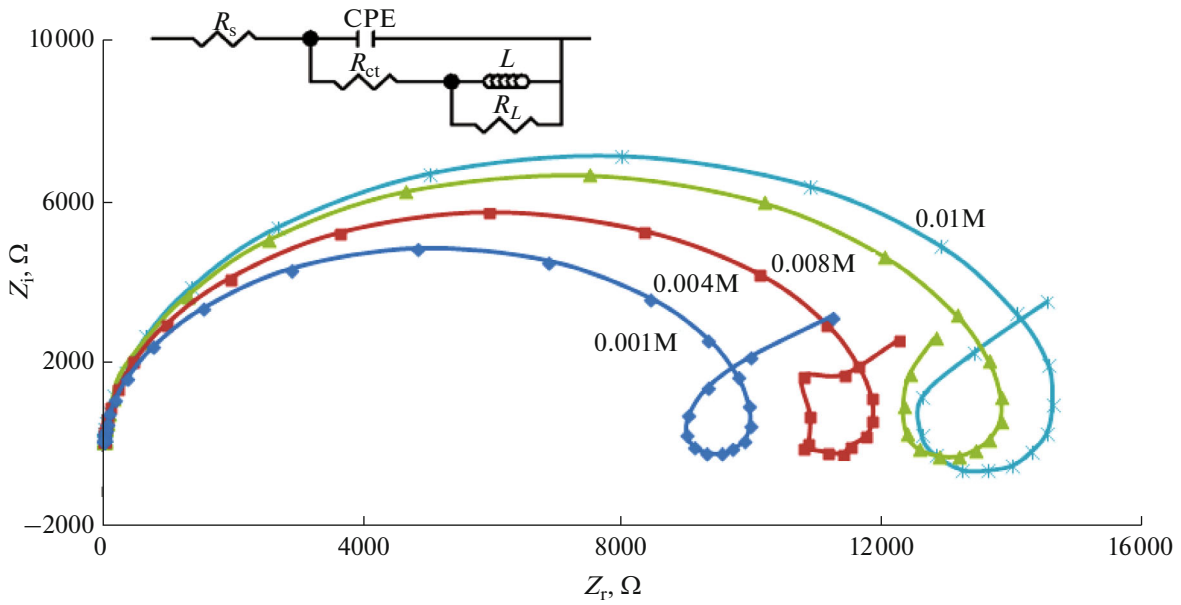


**Fig. 2.** Nyquist plots of Al in 0.5 M $H_2SO_4$ solution containing different concentrations of the inhibitor in different magnification and electrical equivalent circuit.

increased with inhibitor concentration reaching a maximum value of 58.64% at $10^{-3}$ mol/L.

### *3.2. Electrochemical Impedance Spectroscopy*

Electrochemical impedance spectroscopy is one of the best techniques for analyzing the properties of conducting polymer electrodes and charge transfer mechanism in the electrolyte/electrode interface. This has been broadly discussed in the literature using a variety of theoretical models [23–34]. Impedance measurements were performed under potentiostatic conditions after 1 h of immersion. Nyquist plots of uninhibited and inhibited solutions containing different concentrations of inhibitor molecules were performed over the frequency range from 100 to 100 mHz and are shown in Fig. 2. The similarity in the shapes of these graphs throughout the experiment indicates that the addition of inhibitor molecules does not cause any noticeable change in the corrosion mechanism [22]. The Nyquist diagrams show one capacitive loop at high frequencies. The capacitive loop at high frequencies represents the phenomenon associated with the electrical double layer. The above impedance diagrams (Nyquist) contain depressed semicircles with the centre under the real axis. Such behavior is characteristic of solid electrodes and often referred to as frequency dispersion, attributed to different physical phenomena such as roughness, inhomogeneities of the solid surfaces, impurities, grain boundaries, and distribution of surface active sites. The ideal capacitive behavior is not observed in this case and hence a constant phase element CPE is introduced in the circuit to give a more accurate fit [35–37]. The simplest equivalent circuit is represented in Fig. 2, which is a parallel combination of the charge transfer resistance ($R_{ct}$) and the constant phase element (CPE), both in series with the solution resistance ($R_s$). The impedance function of a CPE can be represented as:

$$Z_{CPE} = Y_0^{-1}(j\omega)^{-n}, \quad (3)$$

where $Y_0$ is the CPE constant, ω is the angular frequency, and n is the CPE exponent, which can be used as a gauge of the heterogeneity or roughness of the surface [25, 26]. In the present work, the value of n has a tendency to decrease with increasing inhibitor concentration, which may be attributed to the increase of inhibitor concentration resulted in the increasing surface roughness. For a circuit including a CPE, the $C_{dl}$ could be calculated from CPE parameter values $Y_0$ and $n$ using the expression [22]:

$$C_{dl} = Y_0 (\omega''_m)^{-n}, \quad (4)$$

where $C_{dl}$ is the double layer capacitance and $\omega''_m$ is the frequency at which the imaginary part of the impedance has a maximum. As seen in Table 2, the double layer capacitance ($C_{dl}$) decreases with increase in concentration. This can be attributed to the gradual replacement of water molecules by the adsorption of the organic molecules at metal/solution interface, which is leading to a protective film on metal surface. In addition, the more the inhibitor is adsorbed, the more the thickness of the barrier layer increases according to the expression of the Helmholtz model [35]:

$$C_{dl} = \frac{\varepsilon\varepsilon_0 A}{d}, \quad (5)$$

**Table 2.** Impedance parameters for the corrosion of Al in 0.5M $H_2SO_4$ containing different concentration of 4-IPhOXTsat 298 K

| Concentration, M | $R_s$, Ω | $Y_0$, $\mu\Omega^{-1} s^n cm^{-2}$ | $n$ | $R_L$, Ω | $R_p$, Ω | $L$ (H) | $C_{dl}$, μF $cm^{-2}$ |
|---|---|---|---|---|---|---|---|
| 0 | 1.15 | 187.14 | 0.97 | | 5285 | | 174.11 |
| $2.0 \times 10^{-4}$ | 1.28 | 145.58 | 0.92 | 985 | 11852 | 17.14 | 128.18 |
| $4.0 \times 10^{-4}$ | 1.78 | 1.1.64 | 0.89 | 1385 | 12350 | 68.982 | 85.65 |
| $6.0 \times 10^{-4}$ | 1.98 | 82.17 | 0.88 | 2187 | 13654 | 142.75 | 58.14 |
| $8.0 \times 10^{-4}$ | 2.14 | 72.85 | 0.86 | 2720 | 14850 | 287.45 | 42.57 |
| $1.0 \times 10^{-3}$ | 2.36 | 58.19 | 0.82 | 3095 | 15987 | 412.85 | 32.38 |

where $d$ is the thickness of the protective layer, e is the dielectric constant of the medium, $\varepsilon_0$ is the vacuum permittivity and A is the surface area of the electrode. The equation used for calculating the percentage inhibition efficiency is:

$$\eta(\%) = 100\left(\frac{R_{ct}^* - R_{ct}}{R_{ct}^*}\right), \quad (6)$$

where $R_{ct}^*$ and $R_{ct}$ are values of the charge transfer resistance observed in the presence and absence of inhibitor molecules. Impedance parameters are summarized in Table 2. The results obtained from the EIS technique in acidic solution were in good agreement with those obtained from the polarization method. As observed in Table 2, the adsorption of 4-IPhOXTs-molecules on Al surface modifies the interface between the corrosive medium and metal surface and decreases its electrical capacity. The increase in $R_{ct}$ values with increase in 4-IPhOXTsconcentration can be interpreted as the formation of an insulated adsorption layer. At the highest inhibitor concentration of $10^{-3}$ mol/L, the inhibition efficiency markedly increases and reaches 66.94%. Thus, it can be deduced that 4-IPhOXTshas a clear role in metal protection at the concentration of $10^{-3}$ M.

### *3.3. Weight Loss Measurements*

At different temperatures (298–318 K), the results of weight loss measurements in 0.5 M $H_2SO_4$ solution without and with different concentrations of 4-IPhOXTsare shown in Table 3. The corrosion rate of Al was determined using the relation

$$W = \frac{\Delta m}{St}, \quad (7)$$

where $\Delta m$ is the mass loss, $S$ the area and $t$ is the immersion period. The inhibition efficiencies, IE(%), were calculated by the following equation:

$$\text{IE}\ (\%) = \left(\frac{W_0 - W}{W_0}\right) \times 100, \quad (8)$$

**Table 3.** Results of weight loss test of 4-IPhOXT inhibitor with different concentration

| Inhibitor concentration, M | Corrosion rate, mg $cm^{-2} h^{-1}$ (298 K) |
|---|---|
| 0 | 4.15 |
| $2.0 \times 10^{-4}$ | 2.97 |
| $4.0 \times 10^{-4}$ | 2.33 |
| $6.0 \times 10^{-4}$ | 2.14 |
| $8.0 \times 10^{-4}$ | 1.85 |
| $1.0 \times 10^{-3}$ | 1.62 |

$W_0$ and $W$ are the corrosion rates in the absence and presence of the inhibitors, respectively. From Table 3, it can be found that as temperature increases, the corrosion rate improves and IE (%) reduces. This phenomenon might be attributed to the fact that higher temperature could speed up hot movement of the organic molecules and weaken the adsorption ability of inhibitor on metal surface. It can also be seen in Table 3 that the increase in inhibitor concentration leads to an increase in inhibition efficiency and a decrease in corrosion rate. This result suggests that plenty of adsorbed inhibitor molecules move onto the metal surface. Then, the contact area between metal surface and aggressive solution becomes smaller and smaller leading to the decrease in active sites. The inhibition efficiency obtained by weight loss measurements is lower than that from electrochemical experiments. This difference is attributed to weight loss experiments giving average corrosion rates, whereas the electrochemical experiments give instantaneous corrosion rates. Therefore, the discrepancy in inhibition efficiency obtained by the two methods is understandable. However, the trend in inhibition efficiency with increasing inhibitor concentration is similar regardless of the selection of electrochemical or weight loss method. The inhibition efficiency increases as inhibitor concentration increases.

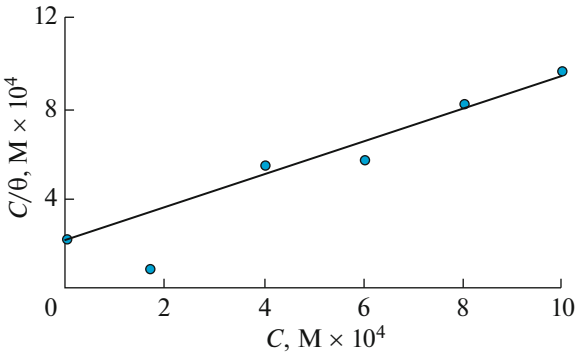


**Fig. 3.** Langmuir adsorption plot for Al in 0.5 M $H_2SO_4$ containing different concentrations of 1,4-Ph(OX)$_2$(Ts)$_2$.

### *3.4. Adsorption Isotherms*

The adsorption of an organic adsorbate at metal/solution interface can be presented as a substitution adsorption process between the organic molecules in aqueous solution, ($Org_{aq}$), and the water molecules on metallic surface, ($H_2O_{ads}$) $Org_{aq}$

$$Org_{aq} + XH_2O_{ads} \leftrightarrow Org_{ads} + XH_2O_{aq}, \qquad (9)$$

where $X$, the size ratio, is the number of water molecules displaced by one molecule of organic inhibitor. $X$ is assumed to be independent of coverage or charge on the electrode [36]. Basic information on the interaction between the inhibitors and the steel surface is provided by the adsorption isotherm. The degree of surface coverage, θ, at different inhibitor concentrations in 0.5 M $H_2SO_4$ was evaluated from weight loss measurements (θ = IE (%)/100) at 25°C. The plot of $C/\theta$ against inhibitor concentration, C, displayed a straight line for the tested inhibitor (Fig. 3). The linear plot clearly revealed that the surface adsorption process of 4-IPhOXTson the Al surface obeys the Langmuir isotherm. Likewise, it suggests that an adsorption process occurs, which can be expressed as follows [37]:

$$\frac{C}{\theta} = \frac{1}{K_{ads}} + C, \qquad (10)$$

where $K_{ads}$ is the equilibrium constant of the adsorption process. Free energy of adsorption ($\Delta G_{ads}$) can be calculated by Eq. (11). The numeral of 55.5 is the molar concentration of water in the solution:

$$K_{ads} = \frac{1}{55.5}\exp\left(\frac{-\Delta G^0_{ads}}{RT}\right). \qquad (11)$$

The value of $\Delta G^0$ ads for adsorption of 4-IPhOXTswas found to be −9.18 kJ mol$^{-1}$. The negative value of $\Delta G^0$ ads suggests that 4-IPhOXTsis spontaneously adsorbed on the Al surface. Literature survey reveals that the values of $\Delta G^0$ ads around −20 kJ mol$^{-1}$ or lower are consistent with the electrostatic interaction between the charged molecules and the charged metal (physical adsorption) [38]. The adsorption of an inhibitor on the metal surface can occur on the basis of donor-acceptor interactions between the *p*-electrons of the heterocyclic compound and the vacant *d*-orbitals of the metal surface atoms. Therefore, the energies of the frontier orbitals should be considered. Energy of LUMO shows the ability of the molecule to receive charge when attacked by electron pair donors, even as the energy of HOMO to donate the charge when attached by electron seeking reagents. As the energy gap between the frontier orbitals gets smaller, the interactions between the reacting species strengthen [39]. In this regard, the electronic properties such as highest occupied molecular orbital (HOMO) energy, lowest unoccupied molecular orbital (LUMO) energy and frontier molecular orbital coefficients have been calculated for prepared inhibitor. Results are presented in Fig. 4 and Table 4. According to the results, HOMO location in the 4-IPhOXTs molecule is mostly distributed in the vicinity of the nitrogen, oxygen atoms. This indicates the reactive sites of the interaction between 4-IPhOXTs and the Al surface. Mulliken population analysis, presented in Fig. 4e, is further evidence for the interaction between Al surface and inhibitor active sites. It is clear from Fig. 4 that the nitrogen atoms of 4-IPhOXTs have considerable excess of negative charge than other atoms. Thus, the adsorption of 4-IPhOXTs as a neutral molecule on the metal surface can occur directly involving the displacement of water molecules from the metal surface and sharing of electrons between the nitrogen atoms and the metal surface. It should be noted that 4-IPhOXTs adsorbs mainly through electrostatic interactions between the positively charged nitrogen atom (since acidic solution can protonate the nitrogen atoms of 4-IPhOXTs and the negatively charged metal surface (physisorption) as evident in the value of $\Delta G^0_{ads}$ obtained.

**Table 4.** Orbital energies for HOMO, LUMO, HOMO-LUMO gap energy ($\Delta E$) and dipole moment (μ) of 4-IPhOXTsin the gaseous (G) and aqueous (A) phases*

| Phase | $E_{HOMO}$, eV | $E_{LUMO}$, eV | $\Delta E$, eV | μ, D |
|---|---|---|---|---|
| G | −5.533 | −1.321 | 4.212 | 8.7507 |
| A | −5.532 | −1.322 | 4.210 | 8.7512 |

* All quantum chemical parameters calculated at DFT level using the 6-31G(d,p) basis set

## 4. CONCLUSION

4-IPhOXTs was found to inhibit the corrosion of Al in 0.5 M $H_2SO_4$ solution and the extent of inhibition was concentration dependent. Inhibition efficiency increases with increasing inhibitor concentration. EIS plots indicate that the charge transfer resistances increase

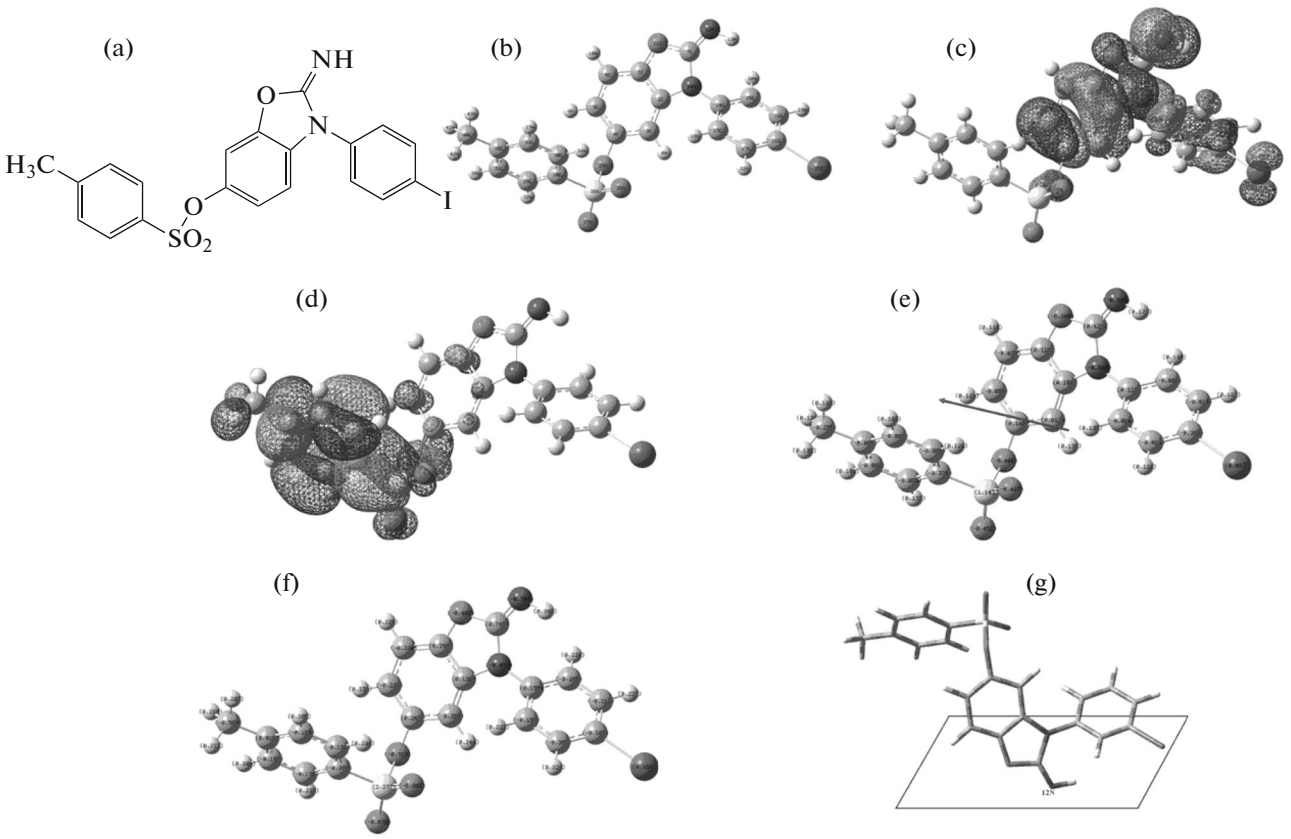


**Fig. 4.** a—Structure of 1,4-Ph$(OX)_2(Ts)_2$; b—optimized molecular structure of 1,4-Ph$(OX)_2(Ts)_2$, H atoms have been omitted for clarity; c—the highest occupied molecular orbital (HOMO) of 1,4-Ph$(OX)_2(Ts)_2$; d—the lowest unoccupied molecular orbital (LUMO) of 1,4-Ph$(OX)_2(Ts)_2$; e—muliken charge population analysis and vector of dipole moment of 1,4-Ph$(OX)_2(Ts)_2$; f—natural charge population analysis of 4-IPhOXTs and g—the schematic representation of the adsorption behavior of 4-IPhOXTson the surface of the Al.

with increasing concentration of the inhibitor at the highest inhibitor concentration of $10^{-3}$ mol/L, the inhibition efficiency increases. 4-IPhOXTs inhibits corrosion by getting adsorbed on the metal surface following Langmuir adsorption isotherm. Quantum chemical calculations show that the adsorption sites are mainly located around the nitrogen atoms of 4-IPhOXTs.

## ACKNOWLEDGMENTS

We gratefully acknowledge the support of this work by Qom University Research Council.

## REFERENCES

1. Ahamad, I. and Quraishi, M.A., *Corros. Sci.,* 2009, vol. 51, p. 2006.
2. Zhang, Q.B. and Hua, Y.X., *Electrochim. Acta,* 2009, vol. 54, p. 1881.
3. Li, W., He, Q., Pei, C., and Hou, B., *Electrochim. Acta,* 2007, vol. 52, p. 6386.
4. Solmaz, R., Kardas, G., Yazıcı, B., and Erbil, M., *Prot. Mater.,* 2005, vol. 41, p. 581.
5. Kardas, G., *Mater. Sci.,* 2005, vol. 41, p. 337.
6. Aljourani, J., Raeissi, K., and Golozar, M.A., *Corros. Sci.,* 2009, vol. 51, p. 1836.
7. Zheludkevich, M.L., Yasakau, K.A., Poznyak, S.K., and Ferreira, M.G.S., *Corros. Sci.,* 2005, vol. 47, p. 3368.
8. Obot, I.B., Obi-Egbedi, N.O., and Umoren, S.A., *Corros. Sci.,* 2009, vol. 51, p. 276.
9. Hosseini, M.G., Ehteshamzadeh, M., and Shahrabi, T., *Electrochim. Acta,* 2007, vol. 52, p. 3680.
10. Afak, S.S., Duran, B., Yurt, A., and Turkoglu, G., *Corros. Sci.,* 2012, vol. 54, p. 251.
11. Hassan, H.H., Adbelghani, E., and Amin, M.A., *Electrochim. Acta,* 2007, vol. 52, p. 6359.
12. Abdoud, Y., Abourrriche, A., Saffaj, T., et al., *Mater. Chem. Phys.,* 2007, vol. 105, p. 1.
13. Quaraishi, M.A., Rawat, J., and Ajmal, M., *J. Appl. Electrochem.,* 2000, vol. 30, p. 745.
14. Khaled K.F. , Amin M.A., Corros. Sci. 2009. V.51. P.1964.

15. Obot, I.B. and Obi-Egbedi, N.O., *Corros. Sci.,* 2010, vol. 52, p. 282.
16. Habibi, D., Nasrollahzadeh, M., Sahebekhtiari, H., et al., *Tetrahedron,* 2013, vol. 69, p. 3082.
17. Kokalj, A., *Electrochim. Acta,* 2010, vol. 56, p. 745.
18. *Gaussian View, V. 3.0,* Pittsburgh, PA: Gaussian, 2003.
19. Reed, A. and Weinhold, F., *Chem. Rev.,* 1998, vol. 88, p. 899.
20. Schelegel, H.B. *Ab Initio Methods in Quantum Chemistry,* New York: Wiley, 1987.
21. Mahjani, M., Moshrefi, R., Ehsani, A., and Jafarian, M., *Anti-Corros. Methods Mater.,* 2011, vol. 58, p. 250.
22. Zhihua, T., Shengtao, Z., Weihua, L., and Baorong, H., *Ind. Eng. Chem. Res.,* 2011, vol. 50, p. 6082.
23. Ehsani, A., Mahjani, M., and Jafarian, M., *Turk. J. Chem.,* 2011, vol. 35, p. 1.
24. Ehsani, A., F. Babaei, and Nasrollahzadeh M., *Appl. Surf. Sci.,* 2013, vol. 283, p. 1060.
25. Ehsani, A., Mahjani, M., Jafarian, M., and Naeemy, A., *Electrochim. Acta,* 2012, vol. 71, p. 128.
26. Ehsani, A., Mahjani, M., Jafarian, M., and Naeemy, A., *Prog. Org. Coat.,* 2010, vol. 69, p. 510.
27. Ehsani, A., Mahjani, M.G., and Jafarian, M., *Synth. Met.,* 2011, vol. 161, p. 1760.
28. Hassan, H., *Electrochim. Acta,* 2006, vol. 51, p. 5966.
29. Martinez, S., *Mater. Chem. Phys.,* 2002, vol. 77, p. 97.
30. Hohenberg, P. and Kohn, W., *Phys. Rev. A,* 1964, vol. 136, p. 864.
31. Obot, I.B., Obi-Egbedi, N.O., and Umoren, S.A., *Corros. Sci.,* 2009, vol. 51, p. 1869.
32. Ozcan, M., Karadag, F., and Dehri, I., *Acta Phys. Chim. Sin.,* 2008, vol. 24, p. 1387.